Design of a Minimal Polypeptide Unit for Bacteriochlorophyll Binding and Self-Assembly Based on Photosynthetic Bacterial Light-Harvesting Proteins†

Dror Noy*,‡ and P. Leslie Dutton

Johnson Research Foundation, Department of Biochemistry and Biophysics, University of Pennsylvania, Philadelphia, Pennsylvania 19104

Received October 24, 2005; Revised Manuscript Received December 21, 2005

ABSTRACT: We introduce LH1β24, a minimal 24 amino acid polypeptide that binds and assembles bacteriochlorophylls (BChls) in micelles of octyl β-glucoside (OG) into complexes with spectral properties that resemble those of B820, a universal intermediate in the assembly of native purple bacterial light-harvesting complexes (LHs). LH1β24 was designed by a survey of sequences and crystal structures of bacterial LH proteins from different organisms combined with currently available information from in vitro reconstitution studies and genetically modified LHs in vivo. We took as a template for the design sphβ31, a truncated 31 amino acid analogue of the native β-apoprotein from the core LH complex of *Rhodobacter sphaeroides*. This peptide self-assembles with BChls to form B820 and, upon cooling and lowering OG concentration, forms red-shifted B850 spectral species that are considered analogous to native LH complexes. We find that LH1β24 self-assembles with BChl in OG to form homodimeric B820-type subunits comprising two LH1β24 and two BChl molecules per subunit. We demonstrate, by modeling the structure using the highly homologous structure of LH2 from *Rhodospirillum molischianum*, that it has the minimal size for BChl binding. Additionally, we have compared the self-assembly of sphβ31 and LH1β24 with BChls and discovered that the association enthalpies and entropies of both species are similar to those measured for native LH1 from *Rhodospirillum rubrum.* However, sphβ31 readily aggregates into intermediate higher oligomeric species and further to form B850 species; moreover, the assembly process of these oligomers is not reversible, and they are apparently large nonspecific BChl−peptide coaggregates rather than well-defined nativelike LH complexes. Similar aggregates were observed during LH1β24 assembly, but these were formed less readily and required lower temperatures than sphβ31. In view of these results, we reevaluate previous in vitro reconstitution studies and propose alternative templates for new designs.

The design and synthesis of customized functional proteins hold great promise for new catalytic systems with selectivity, efficiency, and stereospecificity characteristic of natural enzymes. Making catalytic devices from amino acids provides unique advantages over small synthetic organic and inorganic molecules, including the relatively inexpensive production through expression in bacterial systems, high yield, and high purity as well as considerable versatility and adaptability to various construction requirements and external conditions. This laboratory introduced the concept of protein maquettes (*1*) as flexible, minimal working scaffolds in which to study a selected function abstracted from highly complex natural proteins. Primarily, we focused on one of the most fundamental biocatalytic reactions, the transfer of energy, electrons, and protons in the photosynthetic and respiratory cycles (*2*−*11*), and our success prompted us to apply the lessons learned to create maquettes that will support conversion of light energy into redox/charge separation energy. Recently, we surveyed the extensive database of structural and kinetic information from photosynthetic enzymes and concluded that the basic physics of the transfer processes, namely, the time constraints imposed by the rates of incoming photon flux, and the various decay processes allow for a large degree of tolerance in the engineering parameters (*12, 13*). Additionally, we found that the requirements to guarantee energy and electron transfer rates yielding high efficiency in natural photosystems are largely met by control of distance between chromophores and redox cofactors.

Unfortunately, useful constructions require accommodating dense arrays of different cofactors, some well within 1 nm from each other, within multicofactor transmembranal protein complexes. This type of system still presents the toughest challenge for protein design because our understanding of the principles that underlie structure and folding of membrane proteins lags significantly behind our understanding of water-soluble ones (*14*). This is partly because the emergence of high-resolution structural information about native membrane proteins is relatively recent and confined to many fewer structural examples and because, unlike water-soluble proteins in which the hydrophobic effect dominates folding, membrane protein structures are defined by what appears to

† The authors acknowledge financial support from NIH Grant GM48130, NSF Grant DMR00-79909, and DOE Grant DE-FG02-05ER46223 to P.L.D. and a Human Frontiers Science Program Organization long-term fellowship to D.N.

* To whom correspondence should be addressed. E-mail: dror.noy@weizmann.ac.il.

‡Current address: Department of Structural Biology, Weizmann Institute of Science, Rehovot 76100, Israel. Tel: 972 8 934 2525. Fax: 972 8 934 4185.

10.1021/bi052175x CCC: $33.50
Published on Web 01/25/2006

be a balance between weak interactions for which a usefully clear understanding of assembly has not yet been delineated (*15*).

Clearly, in the case of light-harvesting (LH)[1] proteins, interactions between cofactors also contribute significantly to the assembly process of the whole protein−cofactor complex (*16*, *17*); hence the absence of useful guidelines impacts the decisions regarding how these peptides will fold, self-assemble, and incorporate cofactors. Prior to and even after binding, there are complicated practical issues regarding a more favored cofactor self-aggregation as a result of their own hydrophobicity. And once bound, other complications arise from the multiple possibilities and many degrees of freedom involved in intercofactor and cofactor−protein interactions. Yet, despite our limited understanding of membrane protein folding and assembly which is currently insufficient for designing LH protein maquettes from scratch, it is still possible to start by following the known principles of synthetic membrane protein assembly, utilizing our knowledge and experience with water-soluble maquettes, and drawing inspiration from the features of membrane proteins with known 3D structure.

It is remarkable and fortunate that natural LH proteins, and reaction centers (RCs), currently represent a significant fraction of the membrane proteins that have so far been structurally determined to near-atomic resolution (*17*−*28*). Unlike our previously designed heme-binding protein maquettes that abstracted features of large and complex photosynthetic and respiratory redox proteins (*1*), new LH maquettes can be drawn from the highly symmetric purple bacterial LH proteins which utilize multiple copies of simple α-helical protein subunits to direct and control the self-assembly and organization of large arrays of photosynthetic pigments. Notwithstanding this apparent simplicity and redundancy, complete bottom-up de novo design of a purple bacterial LH maquette is greatly challenged by the increased degrees of freedom associated with such a multicomponent system of proteins, pigments, and lipid or detergent molecules. Therefore, given the extensive database of structural information from crystallographic data, in vivo mutagenesis, and in vitro reconstitution studies (see below), a top-down approach using the native proteins as a template for a new design is expected to be more productive.

The pioneering work of Loach, Parkes-Loach, and colleagues established a protocol for reconstituting purple bacterial LH core complexes (LH1) from their isolated pigment and apoprotein components in micelles of octyl β-glucoside (OG) (*29*). This reconstitution process is conveniently monitored by following the characteristic changes in the absorption and circular dichroism (CD) spectra of bacteriochlorophylls (BChls) as they self-assemble with apoproteins to form the LH complex. In the series of studies that followed, the assembly of various native and modified LH apoproteins was assayed either by enzymatic cleavage or by solid-phase peptide synthesis with BChl and its analogues (*30*−*34*). These, together with mutagenesis studies (*35*−*40*) and the available crystal structures, have provided a detailed account of the critical requirements and the important protein−pigment interactions for self-assembly of natural purple bacterial LH proteins. Loach, Parkes-Loach, and colleagues demonstrated that several cleaved natural α- and β-apoproteins self-assemble with BChls into $\alpha_x\beta_y$BChl$_z$, $\alpha_x\alpha_y$BChl$_z$, or $\beta_x\beta_y$BChl$_z$ complexes with spectroscopic features that were similar to native bacterial LH complexes. In most of these cases an intermediate was formed with absorbance and CD spectra that are typical of the B820 species observed upon detergent treatment of carotenoid-depleted natural LH1 complexes (*41*). These species have been identified as a protomeric αβBChl$_2$ subunit (*42*−*44*) that can reversibly self-assemble to form the various LH oligomers. In peripheral LH complexes (LH2), B820 species could not be generally identified except in reconstitution of LH2 from *Phaeospirillum* (formerly *Rhodospirillum*) *molischianum* (*34*, *45*). However, the crystal structures of LH2 (*17*, *22*, *25*) as well as spectroscopic and computational studies (*46*, *47*) strongly suggest that LH2 complexes are comprised of similar dimeric subunits. Thus B820 may be considered as a universal building block of purple bacterial LH complexes.

Some of the modified LH proteins could aggregate further and exhibited spectral features characteristic of native LH proteins, whereas others remained at the B820 state (*31*, *32*, *34*). Particularly, cleaving 18 residues from the N-terminal of the β-apoprotein of LH1 from *Rhodobacter sphaeroides* resulted in a 30 amino acid long peptide that self-assembled BChls to form B820 spectral species and upon cooling and reducing detergent concentration formed species with the near-infrared (NIR) absorbance maximum red shifted to 850 nm (B850). This feature was similar to native LH2, but a CD spectrum of these species was unique and resembled neither native LH1 nor LH2. A synthetic, 31 amino acid polypeptide labeled sphβ31 with the same sequence and an additional N-terminal Glu residue was shown to be equivalent to its natural analogue and was considered a minimal structural unit that maintains the self-assembly capabilities of native LH complexes. As such, it was used to explore the effect of specific pigment−protein interactions on complex formation and spectral properties. Nango and colleagues continued along the same lines exploring the binding and assembly of BChl as well as Zn-substituted BChl ([Zn]-BChl) (*48*−*50*), chlorin, and porphyrin derivatives (*51*, *52*) with truncated LH1 apoproteins prepared by solid-phase peptide synthesis and more recently by overexpression in *Escherichia coli* (*53*). However, despite the apparent success of sphβ31 and its analogues in binding and assembling various BChl derivatives, studies did not go beyond reproducing some spectroscopic features of native LH1 and LH2 subunits, and so far, the focus was either on random truncation of the native apoproteins determined mainly by the availability of cleavage sites or on single amino acid substitutions.

Here we take a more rigorous approach to design a minimal 24 amino acid hydrophobic protein based on sphβ31. This protein, LH1β24, was designed by a survey of sequences and crystal structures of bacterial LH proteins from different organisms combined with information from reconstitution studies by the Loach and Parkes-Loach laboratory and studies of genetically modified LHs in vivo. Next, we

[1] Abbreviations: BChl, bacteriochlorophyll; CD, circular dichroism; LH, light harvesting; LH1, purple bacterial light-harvesting core complex; LH2, purple bacterial peripheral light-harvesting complex; NIR, near-infrared; OG, octyl β-glucoside; [Zn]-BChl, zinc-substituted bacteriochlorophyll.

Scheme 1: Protein Maquette Designs Based on Native β-Apoproteins of *R. sphaeroides* LH1 (sphβ48), *Ps. molischianum* LH2 (Molβ45), and the 75% Consensus Sequence of LH1 β-Apoproteins[a]

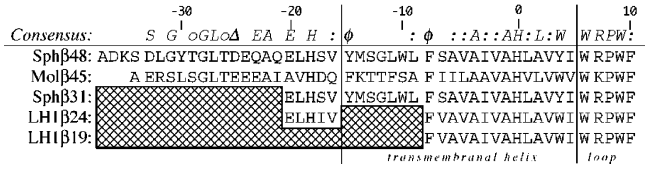

[a] Key: o, hydroxyl residues (S, T); Δ, acidic residues (D, E); ϕ, aromatic residues (F, W, Y); :, hydrophobic residues (I, L, V, A).

follow the self-assembly of LH1β24 and sphβ31 with BChls in OG, compare the spectral features of the intermediate formed during this process, and estimate their oligomeric state and association enthalpies and entropies. Finally, we consider the implications of our results on designing new LH protein maquettes.

MATERIALS AND METHODS

Protein Modeling and Design. For better comparison to previous studies we have adopted the residue numbering convention of Loach and colleagues (*31*). In this scheme residues are numbered relative to the strictly conserved His ligand of BChl, which is designated H-0, with positive numbers toward the C-terminal and negative numbers toward the N-terminal. The crystal structure of the LH2 protein from *Ps. molischianum* (PDB reference 1LGH) (*17*) was used for generating structural models for all other BChl complexes in this study because it is highly homologous to LH1 proteins. In particular, there are 11 residues in the β-chain of this protein that are identical to the sphβ31 sequence, 10 of which are between residues F−8 and F+10 including H-0 and the highly conserved carboxy-terminal motif WRPWF.

Models were generated and refined with the swiss-model set of tools in the modeling software swiss-pdb viewer (available from http://www.expasy.org/spdbv/) and visualized using the program VMD (*54*). The sequence of sphβ31 (Scheme 1) was overlaid on residues −20 to +10 of *Ps. molischianum* LH2 β-polypeptide (molβ45, Scheme 1), and the resulting sphβ31 structure was refined by energy minimization while keeping identical residues fixed at their molβ45 conformation. Inspection of this structure (Figure 1) revealed that the BChl molecule is flanked by phenylalanine, F−8, interacting with the BChl phytyl chain, and tryptophan, W+9, involved in hydrogen bonding to the BChl C3 keto carbonyl group. This region is highly conserved (Scheme 1) whereas residues from position −9 further away from the BChl toward the N-terminus are less conserved and probably less important or unique in establishing binding. Our smallest design was therefore a 19 amino acid peptide, labeled LH1β19 (Scheme 1). This design was highly insoluble in OG, and there was no spectroscopic indication for peptide−BChl interaction. To improve the design, an ELHIV motif was added at the amino-terminus of LH1β19, which included the strictly conserved E−20 and H−18 residues of LH1 β-chains. The addition of another helix turn with polar residues was expected to improve the helix stability and solubility within the detergent micelles. This design was labeled LH1β24 (Scheme 1).

Peptide Synthesis. Peptides were synthesized on Applied Biosystems' Pioneer continuous flow solid-phase synthesizer

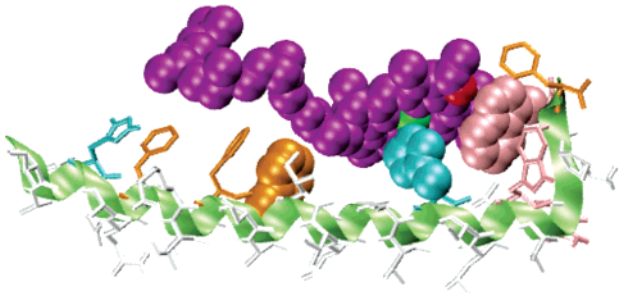

FIGURE 1: Pigment−protein interactions within the binding site of BChl in the natural LH2 β-subunit of *Ps. molischianum* (PDB entry 1LGH). Only 31 amino acid residues from I14 to F45 are shown in stick representation whereas BChl and residues interacting with it are shown in space-filled representation. The protein backbone is shown as a green ribbon with amino acid residues colored gray except histidine, tryptophan, and phenylalanine colored cyan, pink, and orange, respectively. The BChl (purple) is ligated to histidine at its central Mg atom (green) and flanked by a tryptophan hydrogen bonding to its $C3^2$ keto carbonyl oxygen (red) and a phenylalanine interacting with its phytyl chain.

using the standard Fmoc/tBu protection strategy on a Fmoc-PEG-PAL-PS resin (Applied Biosystems) at 0.1 mmol scale. Crude peptides were dissolved in hexafluoroacetone trihydrate (HFA; Aldrich) and purified on a reversed-phase C_{18} HPLC column (Vydac) using gradients of acetonitrile (Fisher) and water, both containing 0.1% (v/v) trifluoroacetic acid (TFA; Sigma). These gradients were similar to those reported by Meadows et al. (*31*) and slightly adjusted for optimal separation. The purity and molecular mass of the HPLC-purified peptides were confirmed by matrix-assisted laser desorption/ionization time-of-flight (MALDI-TOF) mass spectrometry (PerSeptive Biosystems). The measured molecular masses of sphβ31 and LH1β24 were within 1−2 Da from their theoretical values of 3663 and 2873 Da, respectively.

In Vitro Reconstitution. Polypeptides were assembled with pure BChl (kindly provided by Prof. Avigdor Scherz, Weizmann Institute of Science, Israel) according to the procedures described by the Loach laboratory (*31*). Briefly, peptides were solubilized in 5−10 μL of HFA, diluted with 0.5 mL of 4.5% OG (Sigma) solution in 50 mM, pH 7.5, phosphate buffer, and then diluted 5-fold with the same buffer to an OG concentration of 0.9%. An equimolar amount of BChl in ~50 μL of methanol was then added to the solution. Formation of B820 and B850 species was induced by reducing the OG concentration to 0.75% and 0.64%, respectively, and cooling to 4 °C for 2 h in the latter case.

The assembly process of polypeptides and BChls was monitored by absorption and CD spectroscopy with a Cary 5 absorption spectrophotometer and Aviv 202 CD spectrometer, respectively. Temperature dependence experiments were carried out on an Agilent 8453 diode array spectrophotometer equipped with a temperature-controlled sample cell holder. Absorption spectra were automatically recorded 10 min after a temperature point was set. The actual temperature of the sample solution was determined by monitoring absorbance of the thermal sensitive OH overtone band at 966 nm. This transition also features an isosbestic point at 999 nm that was used to correct for baseline offsets. A calibration curve (see Supporting Information) of absorbance changes in 0.9% OG buffer at 966 nm (ΔA) vs temperature changes (ΔT) yielded the linear relation $\Delta T = (0.07 \pm 0.05) + (787 \pm$

4Δ*A*, and the correlation coefficient for a curve consisting of 41 calibration points was 0.999584. To measure an accurate absolute temperature, a blank sample of 0.9% OG buffer solution was equilibrated at 20 °C for 10 min in the cell holder prior to recording a baseline.

Data Analysis and Fitting of Temperature-Dependent Absorption Spectra. Data analysis and curve fitting were performed with Igor Pro 5.0 (Wavemetrics, Lake Oswego, OR) using custom-built scripts and Igor Pro's global fitting package. Temperature-dependent absorbance curves at 780, 820, and 850 nm were globally fitted to models of the general form

$$A(\lambda,T) = \sum_{i}^{N} \epsilon_i(\lambda) C_i(T) \tag{1}$$

where $A(\lambda,T)$ is the absorbance at wavelength λ and temperature T, N is the total number of species, $\epsilon_i(\lambda)$ is the extinction coefficient of a species, i, at wavelength λ, and $C_i(T)$ is the temperature-dependent concentration of this species, which was determined by the specific chemical equilibrium between all of the species in solution. In this work we considered three models of equilibrium between several species of distinct spectral features. For simplicity, we make no assumption about binding monomeric BChl to sphβ31 or LH1β24. Instead, we define the species B780 comprising one BChl and one peptide. The first model describes the self-association of n B780 species into a B820 subunit complex of the form β_nBChl$_n$, where β is either sphβ31 or LH1β24 and is described by the equilibrium equation

$$n\text{B780} \rightleftarrows \text{B820} \qquad K_{1a}(T) = \frac{C_{\text{B820}}}{(C_{\text{B780}})^n} \tag{2a}$$

This model was expanded to describe the formation of B850 species by self-association of m B820 subunits as described by

$$n\text{B780} \rightleftarrows \text{B820} \qquad K_{2a}(T) = \frac{C_{\text{B820}}}{(C_{\text{B780}})^n}$$

$$m\text{B820} \rightleftarrows \text{B850} \qquad K_{2b}(T) = \frac{C_{\text{B850}}}{(C_{\text{B820}})^m} \tag{2b}$$

Alternatively, we considered a model whereby self-association of B820 leads to an intermediate species, B820′, which self-associates further to form the B850 species. For reasons of computational simplicity we assumed B820 and B820′ to be dimers of B780 and B820, respectively, and B850 to comprise m B820′ subunits. The equilibrium equation for this model is thus

$$2\text{B780} \rightleftarrows \text{B820} \qquad K_{3a}(T) = \frac{C_{\text{B820}}}{(C_{\text{B780}})^2}$$

$$2\text{B820} \rightleftarrows \text{B820}' \qquad K_{3b}(T) = \frac{C_{\text{B820}'}}{(C_{\text{B820}})^2}$$

$$m\text{B820}' \rightleftarrows \text{B850} \qquad K_{3c}(T) = \frac{C_{\text{B850}}}{(C_{\text{B820}'})^m} \tag{2c}$$

The concentrations of each species at a given temperature were obtained by solving the equilibrium equations subject to the respective mass balance condition $C_{\text{total}} = \sum_i^N n_i C_i(T)$, where C_{total} is the total peptide concentration and n_i is the stoichiometric constant of each species. Using the integrated form of the van't Hoff equation, we express the temperature-dependent association constants by

$$K_a(T) = C_0 \exp\left[\frac{\Delta H}{R}\left(\frac{1}{T_m} - \frac{1}{T}\right)\right] \tag{3a}$$

where R is the gas constant, T is the temperature in K, ΔH is the standard enthalpy of the reaction, T_m is a typical reaction temperature at which

$$C_i(T_m) = \frac{C_{\text{total}}}{N n_i} \tag{3b}$$

for every i, and C_0 is an integration constant determined by the initial condition of eq 3b. The values ΔH and T_m were determined by fitting the model to the temperature-dependent absorption curves at 780, 820, and 850 nm using ΔH and T_m as global parameters. Once ΔH and $K(T)$ were determined by curve fitting, the entropy change, ΔS, could be determined using the relation

$$\Delta S = \frac{\Delta H - \Delta G}{T} = \frac{\Delta H}{T} + R \ln(K(T)) = \frac{\Delta H}{T_m} + R \tag{3c}$$

Given the optimal set of thermodynamic parameters, it was possible to obtain a least-squares approximation of the spectrum of each species by

$$\mathbf{S}(\lambda_k) = \mathbf{A}(\lambda_k, T_j)\mathbf{C}^+ \tag{4}$$

where **S** is a matrix of pure spectra, **A** is the temperature-dependent spectra arranged in a matrix form in which each column corresponds to a spectrum at a given temperature, and $\mathbf{C}^+$ is the pseudoinverse of the concentration profile matrix **C** in which each row corresponds to a temperature-dependent concentration of a given species as determined by one of the models in eqs 2 and 3.

For comparison with previous reconstitution experiments, we determined the dissociation constants, K_d, of B820 in 0.9% OG using the same method used by the Loach and Parkes-Loach laboratory (*32*). Briefly, we used the equilibrium equation

$$2\text{BChl} + 2\beta \rightleftarrows \text{B820} \qquad K_d = \frac{(C_{\text{BChl}})^2 (C_\beta)^2}{C_{\text{B820}}} \tag{5}$$

where the concentrations of free BChl and B820, C_{BChl} and C_{B820}, respectively, were determined by graphically subtracting a spectrum of free BChl in 0.9% OG from the spectrum of a reconstitution sample at room temperature using extinction coefficients of 55 and 172 $\text{mM}^{-1}\,\text{cm}^{-1}$ for the Q_y absorption maxima of BChl at 778 nm and B820 at 820 nm, respectively (see Supporting Information). The concentration, C_β, of apo-sphβ31 or apo-LH1β24 was determined from the

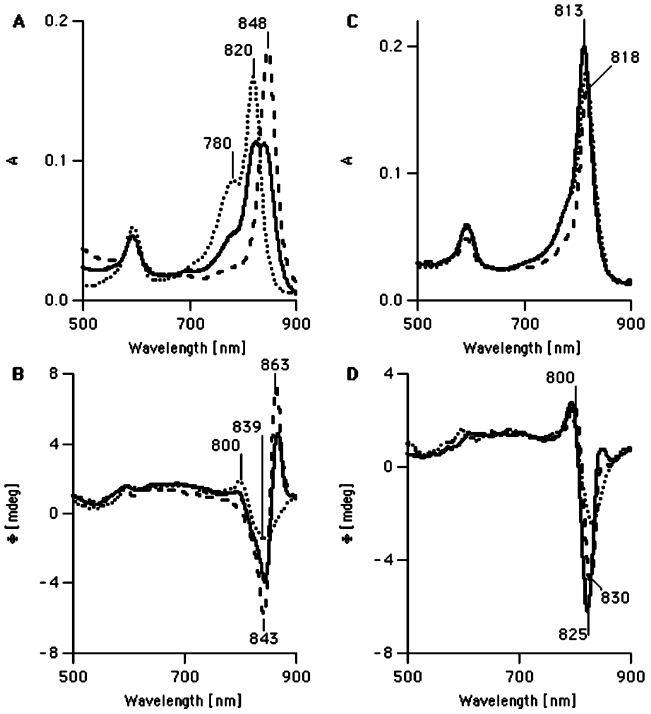

FIGURE 2: Absorbance (A, C) and CD (B, D) spectra of sphβ31 (A, B) and LH1β24 (C, D) in 0.75% (dotted line) and 0.64% (solid line) OG, 50 mM phosphate buffer, pH 7.5 at room temperature, and after 12 h at 4 °C (dashed line). Initial concentrations at 0.9% OG were 4.7 μM sphβ31 and 2.3 μM BChl (A, B) and 9.0 μM LH1β24 and 2.9 μM BChl (C, D).

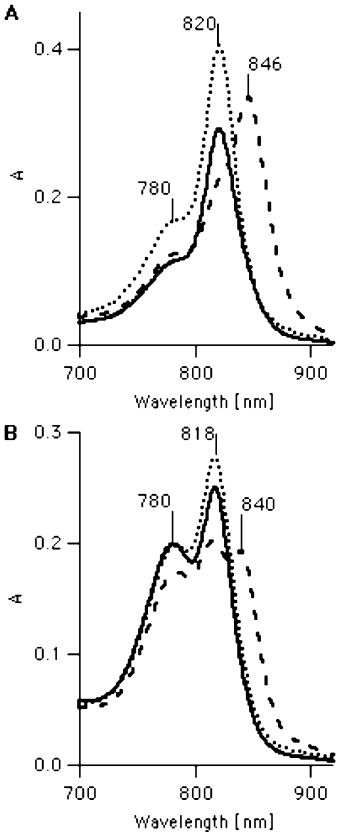

FIGURE 3: Effect of centrifugation on the association and aggregation of sphβ31 (A) and LH1β24 (B) at 0.9% OG and 50 mM phosphate buffer solution, pH 7.5. Peptide and BChl concentrations were 8.0 μM. Solutions composed of mainly B820 species (dotted line) were cooled further until significant amounts of B850 species were observed (dashed line) and then spun in a benchtop centrifuge at 14000 rpm for 20 min (solid line). B850 species formed readily in the sphβ31 sample at 6 °C whereas the LH1β24 required cooling to 2 °C before a significant amount of B850 could be detected.

mass balance equation $C_{total} = C_{\beta} + 2C_{B820}$, where C_{total} is the total protein concentration.

RESULTS

Reconstitution Assays. The absorbance and CD spectra of the various assembly stages of sphβ31 with BChl (Figure 2) are the same as those reported by the Loach and Parkes-Loach laboratory (*30*−*32*): at room temperature in 0.75% OG the NIR absorption maximum of BChl shifts from 780 to 820 nm accompanied by an intense nonconservative CD signal with a small peak at 800 nm and a larger trough at 839 nm. These spectral features are typical of B820, a common intermediate in the assembly and breaking up of LH complexes in carotenoid-deficient strains of purple bacteria, that is considered to comprise a BChl dimer and a heterodimer of native LH polypeptides (*41*). Diluting the sample to an OG concentration of 0.64% and cooling to 4 °C shifted the NIR absorption naximum further to 848 nm accompanied by a more conservative CD signal with a trough at 843 nm and a peak at 863 nm. Similar red shifts to 850 or 870 nm usually accompany the oligomerization of B820 subunits as they form the whole native LH2 or LH1 complexes, respectively (*41*, *43*). Reconstitution of LH1β24 resulted in very similar B820 species at 0.75% OG with a slightly blue-shifted NIR absorption maximum and CD bands compared to sphβ31. However, the absorbance and CD spectra at 0.64% OG did not change significantly except for a 5 nm red shift of the NIR absorption maximum and CD minimum, respectively.

The similarities in absorption spectra between the intermediate and final stages of sphβ31 reconstitution and the respective stages of native LH protein reconstitution in vitro may indicate that both the modified and native polypeptides self-assemble BChls in B820 dimeric units that are organized further into stoichiometrically well-defined LH1- or LH2-type oligomers. In contrast, LH1β24 appears to be capable of assembling BChls only into smaller B820 dimeric subunits. However, the CD spectral features of the sphβ31 B850 complex are significantly different than both the LH1 and LH2 complexes (*41*, *43*, *55*). Most importantly, in native LH1 and LH2 complexes the CD pattern of the lowest energy transition consists of a blue-shifted peak and a red-shifted trough with respect to the position of the absorption maximum whereas sphβ31 exhibits an inverted pattern of a blue-shifted trough followed by a red-shifted peak. The latter pattern is more similar to the CD of BChl aggregates (*56*) although these species exhibit nonconservative CD with a weak blue-shifted trough and an intense red-shifted peak whereas the CD of the sphβ31 B850 species is more conservative with equivalent trough and peak intensities. Additionally, the absorption spectra of the B850 species are accompanied by a significant sloping baseline typical of light scattering by large particles. Thus, it is likely that the B850 species formed by sphβ31 are large coaggregates of peptide and pigments. Indeed, all sphβ31 B850-type complexes were readily sedimented into a firm pellet in a benchtop centrifuge but not B820-type species which remained in the supernatant (Figure 3A). Notably, cooling some LH1β24−BChl prepara-

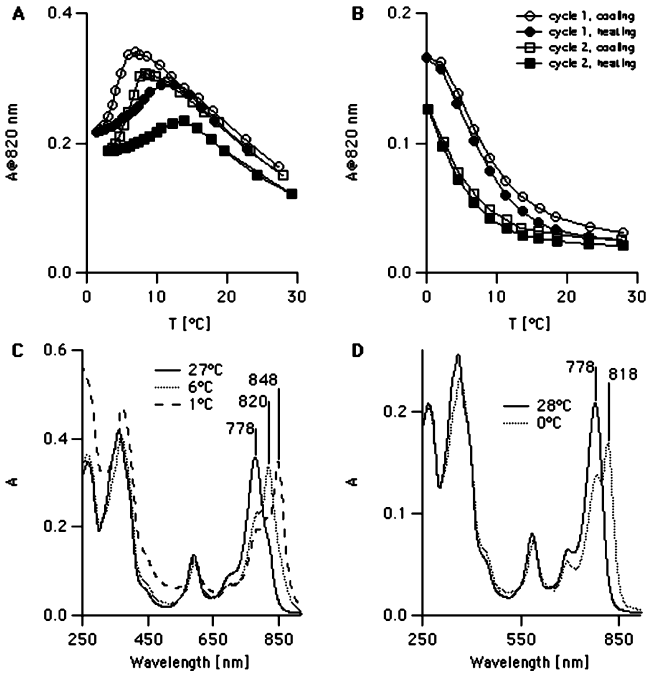

FIGURE 4: Temperature-dependent curves of absorbance at 820 nm of 1:1 (molar ratio) 9.0 μM sphβ31:BChl (A) and 4.7 μM LH1β24:BChl (B) mixtures in 0.9% OG, 50 mM phosphate buffer, pH 7.5, and typical absorption spectra (C and D, respectively) at temperature minima and maxima. An intermediate spectrum at 6 °C is also shown (C).

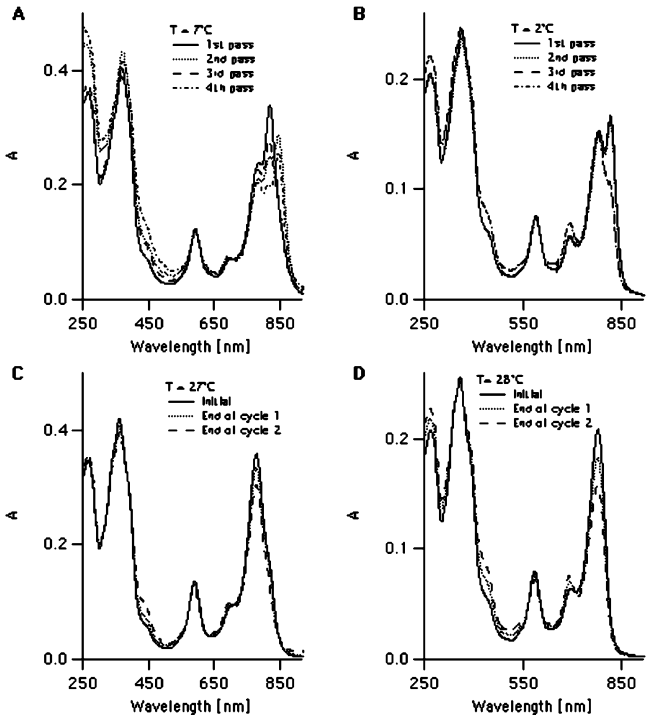

FIGURE 5: Reversibility of assembly assessed by absorption spectra of 1:1 (molar ratio) 9.0 μM sphβ31:BChl (A, C) and 4.7 μM LH1β24:BChl (B, D) mixtures in 0.9% OG and 50 mM phosphate buffer, pH 7.5, at intermediate temperatures (A, B) and end points (C, D) of the scan cycles shown in Figure 4.

tions to approximately 2 °C resulted in a rise of a new absorption band at 840 nm. Similar to sphβ31, benchtop centrifugation completely eliminated this band (Figure 3B), which suggests again that it is due to formation of large BChl aggregates or LH1β24-BChl coaggregates.

Reversibility and Temperature Dependence of sphβ31 and LH1β24 Reconstitution. To further explore the assembly process of sphβ31 and LH1β24 with BChls, we followed the temperature dependence of their absorption spectra in 0.9% OG over two cycles of temperature changes between 28 and 0 °C (Figure 4). These conditions allow cycling through monomeric BChl (B780), subunit-type (B820), and higher oligomeric (B850) species. The assembly of B850 oligomers is clearly nonreversible as indicated by the significant hysteresis in the temperature-dependent curve of absorbance at 820 nm (Figure 4A) and the persistence of the 850 nm absorbance peak during sample warmup. In contrast, the transition from B780 to B820 appears more reversible both in sphβ31 and in LH1β24, and there are only minor differences between cooling and warming the sample to the same temperature during each cycle (Figure 4A,B). These trends are similar to those observed by Pandit et al. (*57*) during assembly and disassembly of native LH1 complexes from *Rhodospirillum rubrum*. Additionally, there are significant differences between the first and second temperature cycle in both peptides, probably because of BChl degradation that occurs during sample warmup. Comparing the spectra at the start and end points of each temperature cycle (Figure 5) reveals a decrease in BChl absorbance at 780 nm and a respective increase in the intensity of two bands at 650 and 420 nm. These features are typical of oxidizing the BChl macrocycle to a chlorophyll macrocycle and are more pronounced in LH1β24 than in sphβ31. This may be a consequence of the BChl being more exposed to the solvent environment because of the smaller size of LH1β24.

Thermodynamic Parameters of sphβ31 and LH1β24 Assembly with BChls. The dissociation constant of sphβ31 B820 at 0.9% OG was determined using eq 5 to be 9.9×10^{-18} M^3, which is only slightly higher than the value of 2.5×10^{-18} M^3 determined by Meadows et al. (*32*). One reason for the discrepancy may be the use of methanol instead of acetone to dissolve the BChl stock. Methanol is known to induce allomerization of BChl to 13^2-OH-BChl, which is capable of forming B820 complexes with sphβ31 but with a different K_d (*58*). Conversely, the K_d value of LH1β24 B820 was determined to be 3.4×10^{-15}, which is significantly higher than that of sphβ31.

The free enthalpies and entropies of sphβ31−BChl and LH1β24−BChl association and oligomerization were obtained by globally fitting temperature-dependent absorbance curves at 780, 820, and 850 nm (Figures 6 and 7, respectively) to the van't Hoff equations (eq 3) that correspond to the assembly schemes described in eq 2. Because of the irreversible nature of the process, only the assembly during the initial cooling stage was considered. Although this stage is not expected to be any more reversible than the overall assembly process, the initial reaction mixture is well-defined because larger aggregates are not formed prior to cooling. The resulting thermodynamic parameters are summarized in Table 1.

Fitting the absorbance curves of sphβ31 to the simplest two-step reaction scheme in eq 2b was unsatisfactory and resulted in nonrandom residuals (not shown). In contrast, the three-step reaction scheme in eq 2c, which assumes an additional intermediate, yielded better fits and more randomly distributed residuals (Figure 6B). The stoichiometric param-

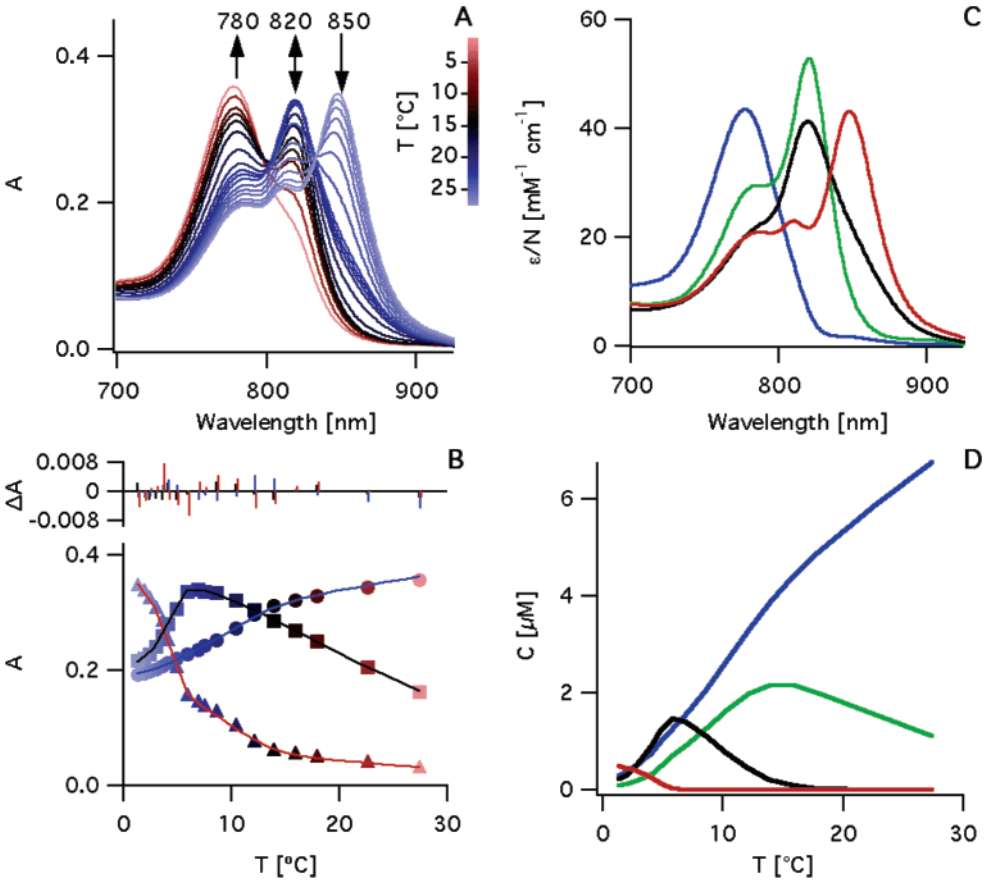

FIGURE 6: Temperature-dependent spectra (A) of a 1:1 (molar ratio) 9.0 μM sphβ31:BChl mixture in 0.9% OG and 50 mM phosphate buffer, pH 7.5, during the first cooling scan. The corresponding absorbances at 780 nm (circles), 820 nm (squares), and 850 nm (triangle) were globally fitted with eq 2c (B). Pure spectral components (C) were derived from the temperature-dependent spectra using eq 4 and the respective concentrations profile of each species (D).

eter, *m*, in eq 2c was determined by fitting the data using integer *m* values from 2 to 8 and the best fit was obtained for $m = 3$. Nevertheless, the individual component spectra obtained by using eq 4 (Figure 6C) were only slightly affected by the choice of *m* and clearly comprised a mixture of spectral components. This suggests that more intermediates are involved in the assembly process which could not be resolved with the given model.

The assembly of LH1β24 could be adequately described by the oligomerization reaction of B780 to form a B820 subunit complex (eq 2a). Nevertheless, the absorbance at 0 °C significantly deviated from the theoretical curve (Figure 7B), probably because of forming large B850-type aggregates. The stoichiometric parameter, *n*, in eq 2a was determined by fitting the data using integer values from 2 to 8, and the best fit was obtained for $n = 2$, indicating the B820 species is indeed a dimeric LH1β24−BChl complex. Furthermore, and unlike sphβ31, the application of eq 4 yielded individual spectral components that are typical of pure B780 and B820 complexes (Figure 7C).

DISCUSSION

The design and assembly of LH1β24 are another demonstration of the protein maquette concept whereby minimal and functionally essential structural motifs from natural proteins are abstracted and assembled in a nonbiological context. Essentially, we reduced the size of the typical native LH subunit by about a half, maintaining only the BChl binding motif which is just long enough to span the length of a BChl macrocycle (Figure 8). This represents a generic minimal version of the protein subunits that form purple bacterial LH complexes. Notably, shorter polypeptides such as LH1β19 (Scheme 1) and sphβ16, a 16-residue polypeptide synthesized by the Loach laboratory (*32*), were incapable of forming B820 complexes with BChls probably because of their high hydrophobicity and limited solubility in OG micelles. Reconstitution assays show that LH1β24 self-assembles with BChls to form a typical B820 subunit complex. Interestingly, the association enthalpy and entropy of the LH1β24−BChl B820 complex, -154 ± 4 kJ/mol and -0.52 ± 0.01 kJ mol^{-1} K^{-1}, respectively, are similar to those of the native LH1 complexes from *Rs. rubrum* in 0.8% OG measured by Pandit et al. to be -216 ± 30 kJ/mol and -0.6 ± 0.1 kJ mol^{-1} K^{-1}, respectively (*57*), and by Sturgis and Robert to be -175 kJ/mol and -0.45 kJ mol^{-1} K^{-1}, respectively (*59*). For sphβ31, our measurements and analysis indicate an equilibrium between dimeric and tetrameric B820 species. The association enthalpies and entropies of these species (Table 1) are also comparable to those of native LH1 and LH1β24 although the stoichiometry and thermodnamic parameters should be taken cautiously because of the irreversible formation of higher aggregation intermediates and the likely possibility of the presence of more intermediates that could not be accounted for by eq 2c.

A robust B820 subunit appears to be a universal intermediate of assembly and dissociation of all bacterial LH

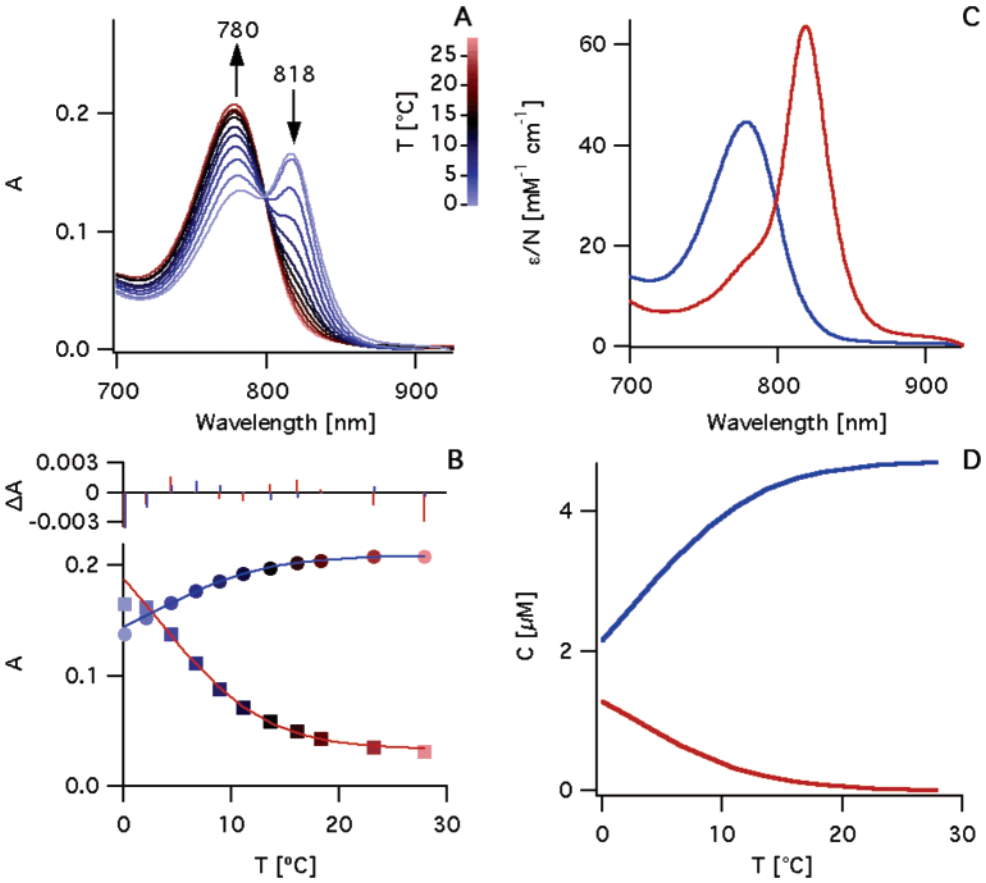

FIGURE 7: Temperature-dependent spectra (A) of a 1:1 (molar ratio) 4.7 μM LH1β24:BChl mixture in 0.9% OG and 50 mM phosphate buffer, pH 7.5, during the first cooling scan. The corresponding absorbances at 780 (circles) and 820 (squares) nm were globally fitted with model 2a (B). Pure spectral components (C) were derived from the temperature-dependent spectra using eq 4 and the respective concentrations profile of each species (D).

Table 1: Thermodynamic Parameters of sphβ31 and LH1β24 Assembly with BChls

peptide	reaction	N_{total}[a]	ΔH (kJ/mol)	T_m (°C)	ΔS (kJ mol^{-1} K^{-1})
sphβ31	2B780 → B820	2	−90 ± 7	9.6 ± 2.5	−0.33 ± 0.03
sphβ31	2B820 → B820′	4	−360 ± 9	9.7 ± 0.5	−1.28 ± 0.03
sphβ31	3B820′ → B850	12	−1423 ± 8	3.80 ± 0.04	−5.14 ± 0.03
LH1β24	2B780 → B820	2	−154 ± 4	1.1 ± 0.8	−0.56 ± 0.02

[a] Total number of monomeric B780 units in the complex.

Scheme 2: Sequence Alignments of LH Proteins Capable of Forming Homooligomeric Complexes with BChl[a]

sphβ48 (*31*):	ADKSDLGYTGLTDEQAQ ELHSV YMSGLWL FSAVAIVAHLAVYIW-RP-W F	−
sphβ31 (*32*):	ELHSV YMSGLWL FSAVAIVAHLAVYIW-RP-W F	*
sphβ35N (*53*):	GCGG ELHSV YMSGLWL FSAVAIVAHLAVYIW-RP-W F	*
sphβ35C (*53*):	G ELHSV YMSGLWL FSAVAIVAHLAVYIW-RP-W FGGC	*
sphβ38 (*53*):	GCGG ELHSV YMSGLWL FSAVAIVAHLAVYIW-RP-W FGGC	*
virβ55 (*31*):	ADLKPSLTGLTEEEAK EFHGI FVTSTVL YLATAVIVHYLVWTA-RP-W IAPIPKGWV	+
virβ39 (*31*):	EFHGI FVTSTVL YLATAVIVHYLVWT**A**-RP-W IAPIPKGWV	+
rrα52 (*31*):	MWRIWQLF DPRQA LVGLATF LFVLALLIHFILLSTERFNW LEGASTKPVQTS	−
rrα43 (*49*):	PRQA LVGLATF LFVLALLIHFILLSTERFNW LEGASTKPVQTS	+
rrα36 (*49*):	CGG DPRQA LVGLATF LFVLALLIHFILLSTERFNW	+

[a] Native sequences of the *Rs. rubrum* α-chain (rrα52) and *R. sphaeroides* and *B. viridis* β-chains (sphβ48 and virβ55) are underlined. Proteins forming either nativelike B870 species or non-native B850 species are marked by + and *, respectively. Neither B850 nor B870 species were observed with native sphβ48 and rrα52 marked by −.

proteins, whether native truncated or modified, and requires only a minimal BChl binding protein such as demonstrated in the LH1β24 maquette. In contrast, there are significant differences in the type and properties of larger BChl−protein oligomers formed by native and modified proteins; for example, neither LH1β24 nor sphβ31 could assemble BChls

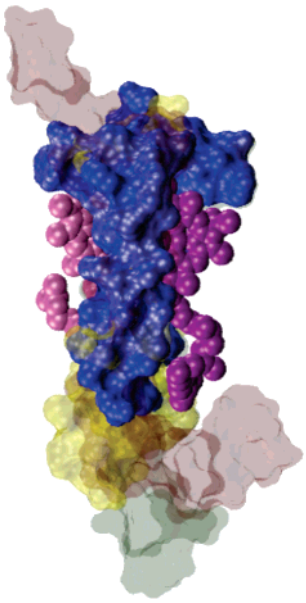

FIGURE 8: 3D homology models of sphβ31 (transparent yellow) and LH1β24 (blue) overlaid on the crystal structure of native LH2 (red and green shades of α- and β-chains, respectively) subunit complexes by aligning the BChls (purple) in each model.

into stoichiometrically well-defined oligomers typical of native purple bacterial LH proteins. Native B820 subunits of LH1 self-assemble into a hexadecamer, and according to Pandit et al. (*57*), the association enthalpies and entropies, e.g., in *Rs. rubrum*, are -2390 ± 450 kJ/mol and 6.3 ± 1.6 kJ mol^{-1} K^{-1}, respectively, which yields enthalpy and entropy of -150 ± 30 kJ/mol and 0.4 ± 0.1 kJ mol^{-1} K^{-1} per B820 subunit, respectively, assuming noncooperative association. These values are almost the same as those measured for individual B820 formation, yet native LH1 association is exergonic with a reaction free energy, ΔG, of -531 kJ/mol at ambient temperature (*57*) whereas we found the association of 12 sphβ31 B820 subunits into B850 species to be endergonic at ambient temperature with a positive ΔG of 93 ± 17 kJ/mol. Thus, although the formation enthalpies and entropies are similar for all B820 subunits, forming stable LH1-type oligomers depends on a finer balance between entropic and enthalpic factors. This notwithstanding, the B850 oligomers formed by sphβ31 and to a lesser extent by LH1β24 are not well-defined oligomeric structures like the native LH1 and LH2 complexes but rather aggregates of B820 subunits.

Previous reconstitution studies have focused on the B850 oligomers of sphβ31 as a model system for understanding how native LH complexes are self-assembled. Most notably, the laboratories of Loach and Parkes-Loach and of Nango prepared and explored a variety of sphβ31 analogues. These included extensions and truncations of the N-terminal (*30*, *32*, *60*) substitutions and chemical modifications of single amino acid residues (*32*, *39*, *60*) and covalent dimerization through disulfide bonds by addition of cysteines at the N- and/or C-termini (*50*, *53*). These studies provided valuable guidelines for the formation of the B820 subunit complex but shifted attention from two additional truncated LH proteins capable of reconstituting homooligomeric BChl complexes (*31*). These 43- and 39-residue truncated α-chains of *Rs. rubrum* (Scheme 2, rrα43) and the β-chain of *Blastochloris viridis* (Scheme 2, virβ39), respectively, exhibited spectroscopic features that were almost identical to native LH1. Interestingly, no B820 intermediate was observed during reconstitution of these species.

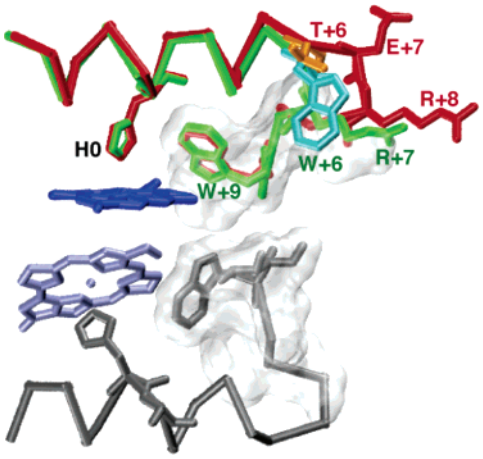

FIGURE 9: Structural alignments of sphβ31 (green) and rrα36 (red) on the β-chain of *Ps. molischianum* (PDB entry 1LGH). This chain is packed against the α-chain of a neighboring B820 subunit (gray) as demonstrated by the white surfaces.

We conclude by reevaluating previous reconstitution studies in view of the present results implicating the B850 species of sphβ31 and its analogues as nonspecific protein−BChl coaggregates. Scheme 2 summarizes the sequences of native and modified LH apoproteins capable of forming homooligomeric complexes with BChls. Obviously, native α- and β-chains of *Rs. rubrum* and *B. viridis*, respectively, differ from the *R. sphaeroides* β-chain in their extended C-terminal sequence. Since similar extensions were shown to be involved in intersubunit interaction in the crystal structures of LH2 (*16*, *17*), they may serve to provide the necessary protein−protein interactions for proper association of the homooligomeric LH1 complex. However, a recent study by Nagata et al. (*49*) showed that truncating the C-terminal sequence of rrα43 (Scheme 2, rrα36) had no effect on its ability to form nativelike LH1 complexes with BChls as well as with [Zn]-BChls. This is surprising because the size of rrα36 is similar to sphβ31 and both have no C-terminal extension beyond the BChl binding motif, yet their self-association properties are markedly different. Nonetheless, closer inspection of the sequences (Scheme 2) and structural alignment of rrα36 and sphβ31 (Figure 9) suggests that the flexibility of the loop region extending from position +6 to +11 or +9 in α- and β-chains, respectively, may be the key to proper association. Notably, the highly conserved tryptophan, W+6, of LH β-chains is replaced by alanine in *B. viridis*. This position connects between the α-helical and loop domains of LH apoproteins, and alanine probably confers more conformational freedom to the loop than tryptophan. Similarly, *Rs. rubrum* α-chains have a threonine in position +6 and a two-residue longer loop connecting to tryptophan, W+11, that forms a hydrogen bond to the BChl C3 keto carbonyl and is equivalent to W+9 in LH β-chains. In the native LH1 complex, the C-terminal loop region of one B820 α-subunit is packed against the β-chain from another subunit, and therefore enhancing the flexibility of these loops may allow for better packing interactions. The verification of this hypothesis will require further investigations of new LH maquettes based not only on sphβ31 but also on rrα36 and virβ39. Such investigations should not

rely exclusively on spectroscopic assays but must obtain direct information about the actual oligomeric state of the LH species in solution. We are currently exploring the possibilities of using analytical ultracentrifugation and light scattering techniques for this purpose.

SUPPORTING INFORMATION AVAILABLE

(1) A calibration curve for the temperature-dependent water absorption band at 966 nm and (2) deconvolution of room temperature spectra of sphβ31 and LH1β24 into free BChl and B820 spectra. This material is available free of charge via the Internet at http://pubs.acs.org.

REFERENCES

1. Robertson, D. E., Farid, R. S., Moser, C. C., Urbauer, J. L., Mulholland, S. E., Pidikiti, R., Lear, J. D., Wand, A. J., Degrado, W. F., and Dutton, P. L. (1994) Design and synthesis of multi-heme proteins, *Nature 368*, 425−431.
2. Chen, X. X., Discher, B. M., Pilloud, D. L., Gibney, B. R., Moser, C. C., and Dutton, P. L. (2002) De novo design of a cytochrome *b* maquette for electron transfer and coupled reactions on electrodes, *J. Phys. Chem. B 106*, 617−624.
3. Discher, B. M., Noy, D., Strzalka, J., Ye, S., Moser, C. C., Lear, J. D., Blasie, J. K., and Dutton, P. L. (2005) Design of amphiphilic protein maquettes: controlling assembly, membrane insertion, and cofactor interactions, *Biochemistry 44*, 12329−12343.
4. Gibney, B. R., Rabanal, F., Reddy, K. S., and Dutton, P. L. (1998) Effect of four helix bundle topology on heme binding and redox properties, *Biochemistry 37*, 4635−4643.
5. Grosset, A. M., Gibney, B. R., Rabanal, F., Moser, C. C., and Dutton, P. L. (2001) Proof of principle in a de novo designed protein maquette: An allosterically regulated, charge-activated conformational switch in a tetra-alpha-helix bundle, *Biochemistry 40*, 5474−5487.
6. Noy, D., Discher, B. M., Rubtsov, I. V., Hochstrasser, R. M., and Dutton, P. L. (2005) Design of amphiphilic protein maquettes: Enhancing maquette functionality through binding of extremely hydrophobic cofactors to lipophilic domains, *Biochemistry 44*, 12344−12354.
7. Sharp, R. E., Moser, C. C., Rabanal, F., and Dutton, P. L. (1998) Design, synthesis, and characterization of a photoactivatable flavocytochrome molecular maquette, *Proc. Natl. Acad. Sci. U.S.A. 95*, 10465−10470.
8. Sharp, R. E., Diers, J. R., Bocian, D. F., and Dutton, P. L. (1998) Differential binding of iron(III) and zinc(II) protoporphyrin IX to synthetic four-helix bundles, *J. Am. Chem. Soc. 120*, 7103−7104.
9. Shifman, J. M., Moser, C. C., Kalsbeck, W. A., Bocian, D. F., and Dutton, P. L. (1998) Functionalized de novo designed proteins: Mechanism of proton coupling to oxidation/reduction in heme protein maquettes, *Biochemistry 37*, 16815−16827.
10. Shifman, J. M., Gibney, B. R., Sharp, R. E., and Dutton, P. L. (2000) Heme redox potential control in de novo designed four-alpha-helix bundle proteins, *Biochemistry 39*, 14813−14821.
11. Tommos, C., Skalicky, J. J., Pilloud, D. L., Wand, A. J., and Dutton, P. L. (1999) De novo proteins as models of radical enzymes, *Biochemistry 38*, 9495−9507.
12. Noy, D., Moser, C. C., and Dutton, P. L. (2005) Design and engineering of photosynthetic light-harvesting and electron-transfer using length, time, and energy scales, *Biochim. Biophys. Acta* (in press).
13. Moser, C. C., Page, C. C., Cogdell, R. J., Barber, J., Wraight, C. A., and Dutton, P. L. (2003) Length, time, and energy scales of photosystems, *Adv. Protein Chem. 63*, 71−109.
14. Chamberlain, A. K., Faham, S., Yohannan, S., and Bowie, J. U. (2003) Construction of helix-bundle membrane proteins, *Adv. Protein Chem. 63*, 19−46.
15. Barker, P. D. (2003) Designing redox metalloproteins from bottom-up and top-down perspectives, *Curr. Opin. Struct. Biol. 13*, 490−499.
16. Prince, S. M., Papiz, M. Z., Freer, A. A., McDermott, G., Hawthornthwaite-Lawless, A. M., Cogdell, R. J., and Isaacs, N. W. (1997) Apoprotein structure in the LH2 complex from *Rhodopseudomonas acidophila* strain 10050: Modular assembly and protein pigment interactions, *J. Mol. Biol. 268*, 412−423.
17. Koepke, J., Hu, X. C., Muenke, C., Schulten, K., and Michel, H. (1996) The crystal structure of the light-harvesting complex II (B800−850) from *Rhodospirillum molischianum*, *Structure 4*, 581−597.
18. Jordan, P., Fromme, P., Witt, H. T., Klukas, O., Saenger, W., and Krauss, N. (2001) Three-dimensional structure of cyanobacterial photosystem I at 2.5 angstrom resolution, *Nature 411*, 909−917.
19. McLuskey, K., Prince, S. M., Cogdell, R. J., and Isaacs, N. W. (2001) The crystallographic structure of the B800−820 LH3 light-harvesting complex from the purple bacteria *Rhodopseudomonas acidophila* strain 7050, *Biochemistry 40*, 8783−8789.
20. Kamiya, N., and Shen, J. R. (2003) Crystal structure of oxygen-evolving photosystem II from *Thermosynechococcus vulcanus* at 3.7-angstrom resolution, *Proc. Natl. Acad. Sci. U.S.A. 100*, 98−103.
21. Liu, Z. F., Yan, H. C., Wang, K. B., Kuang, T. Y., Zhang, J. P., Gui, L. L., An, X. M., and Chang, W. R. (2004) Crystal structure of spinach major light-harvesting complex at 2.72 angstrom resolution, *Nature 428*, 287−292.
22. McDermott, G., Prince, S. M., Freer, A. A., Hawthornthwaite-Lawless, A. M., Papiz, M. Z., Cogdell, R. J., and Isaacs, N. W. (1995) Crystal-structure of an integral membrane light-harvesting complex from photosynthetic bacteria, *Nature 374*, 517−521.
23. Bibby, T. S., Nield, J., Chen, M., Larkum, A. W., and Barber, J. (2003) Structure of a photosystem II supercomplex isolated from *Prochloron didemni* retaining its chlorophyll a/b light-harvesting system, *Proc. Natl. Acad. Sci. U.S.A. 100*, 9050−9054.
24. Ben-Shem, A., Frolow, F., and Nelson, N. (2003) Crystal structure of plant photosystem I, *Nature 426*, 630−635.
25. Papiz, M. Z., Prince, S. M., Howard, T., Cogdell, R. J., and Isaacs, N. W. (2003) The structure and thermal motion of the B800−850 LH2 complex from *Rps. acidophila* at 2.0 Å resolution and 100 K: New structural features and functionally relevant motions, *J. Mol. Biol. 326*, 1523−1538.
26. Roszak, A. W., Howard, T. D., Southall, J., Gardiner, A. T., Law, C. J., Isaacs, N. W., and Cogdell, R. J. (2003) Crystal structure of the RC-LH1 core complex from *Rhodopseudomonas palustris*, *Science 302*, 1969−1972.
27. Camara-Artigas, A., and Allen, J. P. (2004) Comparative analyses of three-dimensional models of bacterial reaction centers, *Photosynth. Res. 81*, 227−237.
28. Deisenhofer, J., Epp, O., Miki, K., Huber, R., and Michel, H. (1985) Structure of the protein subunits in the photosynthetic reaction center of *Rhodopseudomonas viridis* at 3 Å resolution, *Nature 318*, 618−624.
29. Parkes-Loach, P. S., Sprinkle, J. R., and Loach, P. A. (1988) Reconstitution of the B873 light-harvesting complex of *Rhodospirillum rubrum* from the separately isolated alpha-polypeptide and beta-polypeptide and bacteriochlorophyll-A, *Biochemistry 27*, 2718−2727.
30. Kehoe, J. W., Meadows, K. A., Parkes-Loach, P. S., and Loach, P. A. (1998) Reconstitution of core light-harvesting complexes of photosynthetic bacteria using chemically synthesized polypeptides. 2. Determination of structural features that stabilize complex formation and their implications for the structure of the subunit complex, *Biochemistry 37*, 3418−3428.
31. Meadows, K. A., Iida, K., Tsuda, K., Recchia, P. A., Heller, B. A., Antonio, B., Nango, M., and Loach, P. A. (1995) Enzymatic and chemical cleavage of the core light-harvesting polypeptides of photosynthetic bacteria—Determination of the minimal polypeptide size and structure required for subunit and light-harvesting complex-formation, *Biochemistry 34*, 1559−1574.
32. Meadows, K. A., Parkes-Loach, P. S., Kehoe, J. W., and Loach, P. A. (1998) Reconstitution of core light-harvesting complexes of photosynthetic bacteria using chemically synthesized polypeptides. 1. Minimal requirements for subunit formation, *Biochemistry 37*, 3411−3417.
33. Parkes-Loach, P. S., Michalski, T. J., Bass, W. J., Smith, U., and Loach, P. A. (1990) Probing the bacteriochlorophyll binding-site by reconstitution of the light-harvesting complex of *Rhodospirillum rubrum* with bacteriochlorophyll-a analogues, *Biochemistry 29*, 2951−2960.
34. Todd, J. B., Recchia, P. A., Parkes-Loach, P. S., Olsen, J. D., Fowler, G. J. S., McGlynn, P., Hunter, C. N., and Loach, P. A. (1999) Minimal requirements for in vitro reconstitution of the structural subunit of light-harvesting complexes of photosynthetic bacteria, *Photosynth. Res. 62*, 85−98.

35. Kwa, L. G., Garcia-Martin, A., Vegh, A. P., Strohmann, B., Robert, B., and Braun, P. (2004) Hydrogen bonding in a model bacteriochlorophyll-binding site drives assembly of light harvesting complex, *J. Biol. Chem. 279*, 15067−15075.
36. Braun, P., Olsen, J. D., Strohmann, B., Hunter, C. N., and Scheer, H. (2002) Assembly of light-harvesting bacteriochlorophyll in a model transmembrane helix in its natural environment, *J. Mol. Biol. 318*, 1085−1095.
37. Fowler, G. J. S., Sockalingum, G. D., Robert, B., and Hunter, C. N. (1994) Blue shifts in bacteriochlorophyll absorbency correlate with changed hydrogen-bonding patterns in light-harvesting 2 mutants of *Rhodobacter sphaeroides* with alterations at alpha-Tyr-44 and alpha-Tyr-45, *Biochem. J. 299*, 695−700.
38. Fowler, G. J. S., Hess, S., Pullerits, T., Sundstrom, V., and Hunter, C. N. (1997) The role of beta Arg(−10) in the B800 bacteriochlorophyll and carotenoid pigment environment within the light-harvesting LH2 complex of *Rhodobacter sphaeroides*, *Biochemistry 36*, 11282−11291.
39. Olsen, J. D., Sturgis, J. N., Westerhuis, W. H. J., Fowler, G. J. S., Hunter, C. N., and Robert, B. (1997) Site-directed modification of the ligands to the bacteriochlorophylls of the light-harvesting LH1 and LH2 complexes of *Rhodobacter sphaeroides*, *Biochemistry 36*, 12625−12632.
40. Sturgis, J. N., Olsen, J. D., Robert, B., and Hunter, C. N. (1997) Functions of conserved tryptophan residues of the core light-harvesting complex of *Rhodobacter sphaeroides*, *Biochemistry 36*, 2772−2778.
41. Loach, P. A., and Parkes-Loach, P. S. (1995) Structure−function relationships in core light-harvesting complexes (LHI) as determined by charterization of the structural subunit and by reconstitution experiments, in *Anoxygenic Photosynthetic Bacteria* (Blankenship, R. E., Madigan, M. T., and Bauer, C. E., Eds.) pp 437−471, Kluwer Academic Publishers, Dordrecht.
42. Visschers, R. W., Chang, M. C., Vanmourik, F., Parkesloach, P. S., Heller, B. A., Loach, P. A., and Vangrondelle, R. (1991) Fluorescence polarization and low-temperature absorption-spectroscopy of a subunit form of light-harvesting complex-I from purple photosynthetic bacteria, *Biochemistry 30*, 5734−5742.
43. Chang, M. C., Callahan, P. M., Parkesloach, P. S., Cotton, T. M., and Loach, P. A. (1990) Spectroscopic characterization of the light-harvesting complex of *Rhodospirillum rubrum* and its structural subunit, *Biochemistry 29*, 421−429.
44. Wang, Z. Y., Muraoka, Y., Nagao, M., Shibayama, M., Kobayashi, M., and Nozawa, T. (2003) Determination of the B820 subunit size of a bacterial core light-harvesting complex by small-angle neutron scattering, *Biochemistry 42*, 11555−11560.
45. Todd, J. B., Parkes-Loach, P. S., Leykam, J. F., and Loach, P. A. (1998) In vitro reconstitution of the core and peripheral light-harvesting complexes of *Rhodospirillum molischianum* from separately isolated components, *Biochemistry 37*, 17458−17468.
46. Novoderezhkin, V., Monshouwer, R., and van Grondelle, R. (1999) Exciton (de)localization in the LH2 antenna of *Rhodobacter sphaeroides* as revealed by relative difference absorption measurements of the LH2 antenna and the B820 subunit, *J. Phys. Chem. B 103*, 10540−10548.
47. Koolhaas, M. H. C., vanderZwan, G., vanMourik, F., and vanGrondelle, R. (1997) Spectroscopy and structure of bacteriochlorophyll dimers. 1. Structural consequences of nonconservative circular dichroism spectra, *Biophys. J. 72*, 1828−1841.
48. Kashiwada, A., Watanabe, H., Tanaka, T., and Nango, M. (2000) Molecular assembly of zinc bachteriochlorophyll *a* by synthetic hydrophobic 1 alpha-helix polypeptides, *Chem. Lett.*, 24−25.
49. Nagata, M., Nango, M., Kashiwada, A., Yamada, S., Ito, S., Sawa, N., Ogawa, M., Iida, K., Kurono, Y., and Ohtsuka, T. (2003) Construction of photosynthetic antenna complex using light-harvesting polypeptide-alpha from photosynthetic bacteria, *R. rubrum* with zinc substituted bacteriochlorophyll alpha, *Chem. Lett. 32*, 216−217.
50. Nango, M., Kashiwada, A., Watanabe, H., Yamada, S., Yamada, T., Ogawa, M., Tanaka, T., and Iida, K. (2002) Molecular assembly of bachteriochlorophyll a using light-harvesting model 1 alpha-helix polypeptides and 2 alpha-helix polypeptide with disulfide-linkage, *Chem. Lett.*, 312−313.
51. Kashiwada, A., Takeuchi, Y., Watanabe, H., Mizuno, T., Yasue, H., Kitagawa, K., Iida, K., Wang, Z. Y., Nozawa, T., Kawai, H., Nagamura, T., Kurono, Y., and Nango, M. (2000) Molecular assembly of covalently-linked mesoporphyrin dimers with light-harvesting polypeptides, *Tetrahedron Lett. 41*, 2115−2119.
52. Kashiwada, A., Watanabe, H., Mizuno, T., Iida, K., Miyatake, T., Tamiaki, H., Kobayashi, M., and Nango, M. (2000) Structural requirements of zinc porphyrin derivatives on the complex-forming with light-harvesting polypeptides, *Chem. Lett.*, 158−159.
53. Dewa, T., Yamada, T., Ogawa, M., Sugimoto, M., Mizuno, T., Yoshida, K., Nakao, Y., Kondo, M., Iida, K., Yamashita, K., Tanaka, T., and Nango, M. (2005) Design and expression of cysteine-bearing hydrophobic polypeptides and their self-assembling properties with bacteriochlorophyll a derivatives as a mimic of bacterial photosynthetic antenna complexes. Effect of steric confinement and orientation of the polypeptides on the pigment/polypeptide assembly process, *Biochemistry 44*, 5129−5139.
54. Humphrey, W., Dalke, A., and Schulten, K. (1996) VMD: Visual molecular dynamics, *J. Mol. Graphics 14*, 33−38.
55. Georgakopoulou, S., Frese, R. N., Johnson, E., Koolhaas, C., Cogdell, R. J., van Grondelle, R., and van der Zwan, G. (2002) Absorption and CD spectroscopy and modeling of various LH2 complexes from purple bacteria, *Biophys. J. 82*, 2184−2197.
56. Scherz, A., and Rosenbach-Belkin, V. (1989) Comparative-study of optical-absorption and circular-dichroism of bacteriochlorophyll oligomers in Triton X-100, the antenna pigment B850, and the primary donor P-860 of photosynthetic bacteria indicates that all are similar dimers of bacteriochlorophyll-A, *Proc. Natl. Acad. Sci. U.S.A. 86*, 1505−1509.
57. Pandit, A., Visschers, R. W., van Stokkum, I. H. M., Kraayenhof, R., and van Grondelle, R. (2001) Oligomerization of light-harvesting I antenna peptides of *Rhodospirillum rubrum*, *Biochemistry 40*, 12913−12924.
58. Davis, C. M., ParkesLoach, P. S., Cook, C. K., Meadows, K. A., Bandilla, M., Scheer, H., and Loach, P. A. (1996) Comparison of the structural requirements for bacteriochlorophyll binding in the core light-harvesting complexes of *Rhodospirillum rubrum* and *Rhodobacter sphaeroides* using reconstitution methodology with bacteriochlorophyll analogs, *Biochemistry 35*, 3072−3084.
59. Sturgis, J. N., and Robert, B. (1994) Thermodynamics of membrane polypeptide oligomerization in light-harvesting complexes and associated structural-changes, *J. Mol. Biol. 238*, 445−454.
60. Parkes-Loach, P. S., Majeed, A. P., Law, C. J., and Loach, P. A. (2004) Interactions stabilizing the structure of the core light-harvesting complex (LHl) of photosynthetic bacteria and its subunit (B820), *Biochemistry 43*, 7003−7016.

BI052175X